ELSEVIER

Journal of Nuclear Materials 290–293 (2001) 216–219

journal of nuclear materials

www.elsevier.nl/locate/jnucmat

Silicon diffusion in amorphous carbon films

E. Vainonen-Ahlgren [a,*], T. Ahlgren [a], L. Khriachtchev [b], J. Likonen [c], S. Lehto [c], J. Keinonen [a], C.H. Wu [d]

[a] *Department of Physics, Accelerator Laboratory, University of Helsinki, P.O. Box 43, FIN-00014 Helsinki, Finland*
[b] *Laboratory of Physical Chemistry, University of Helsinki, P.O. Box 55, FIN-00014 Helsinki, Finland*
[c] *Chemical Technology, Technical Research Centre of Finland, P.O. Box 1404, FIN-02044 VTT, Finland*
[d] *EFDACSU, Max-Planck-Institute für Plasmaphysik, Boltzmannstrasse 2, D-85748 Garching bei München, Germany*

Abstract

Annealing behavior of implanted silicon in amorphous carbon films deposited by a pulsed arc discharge method was studied. Raman spectroscopy was used to characterize the changes in the bonding structure after annealing. The concentration profiles of Si were measured by secondary ion mass spectrometry (SIMS). The obtained diffusion coefficients resulted in an activation energy of 1.6 ± 0.1 eV and pre-exponential factor of $1.9 \times 10^{4\pm1}$ nm^2 s^{-1}. © 2001 Elsevier Science B.V. All rights reserved.

PACS: 66.30.Jt; 61.72.Ss
Keywords: Diffusion; Silicon; Amorphous carbon; Annealing behavior

1. Introduction

There is a growing interest in the synthesis and study of diamondlike carbon (DLC) films. Semiconducting diamond doped with different impurities is expected to have applications in temperature-resistant and high-performance electronic devices [1,2]. In the next-step fusion device ITER (international thermonuclear experimental reactor), carbon fiber composites are primary candidates for divertor armor materials. In the presence of plasma, redeposition of sputtered carbon particles and formation of carbon-based composite films will take place.

A decrease of the chemical sputtering by a factor of 2–3 in silicon-doped carbon [3] compared to pure carbon makes this material attractive for application in a fusion device. Moreover, Si doping will decrease the baking temperature needed to remove impurities from surfaces. Si is also known to be a good oxygen getter and an impurity which increases thermal conductivity [3]. In spite of this, to our knowledge there are no studies presented in the literature on silicon diffusion in carbon. The purpose of this work was to investigate Si diffusion and structural changes occurring in carbon films during annealing. Secondary ion mass spectrometry (SIMS) and Raman spectroscopy were utilized in the study.

Raman spectra of DLC films measured with excitation at 514.5 nm are typically dominated by broad scattering bands around 1560 cm^{-1} (G line) and 1350 cm^{-1} (D line) that are conventionally attributed to well-localized vibrations in sp^2-coordinated clusters [4]. The low-frequency region (400–800 cm^{-1}) of the Raman scattering is due to interaction between sp^3- and sp^2-bonded networks [5,6]. Graphitization of DLC can straightforwardly be characterized by analyzing the intensity ratio of the D and G lines [4,7], which has been employed to study thermal stability of DLC films [8–14] and the structural modifications under irradiation with energetic heavy ions [15–17].

2. Experimental arrangements

The 500–800 nm thick amorphous DLC films (density 2.6 ± 0.2 g/cm^3) were deposited onto crystalline Si

* Corresponding author. Tel.: +358-9 1914 0010; fax: +358-9 1914 0042.
E-mail addresses: elizaveta.vainonen@helsinki.fi, evainone@beam.helsinki.fi (E. Vainonen-Ahlgren).

PII: S0022-3115(00)00564-X

wafers with pulsed cathodic arc discharge facilities of DIARC-Technology Inc. (Finland). Details of the deposition procedure are described elsewhere [18].

The samples were implanted by 80-keV $^{30}Si^{+}$ ions to a dose of 1×10^{16} ions cm^{-2}. The implantations were performed at room temperature in the 120-keV isotope separator of the University of Helsinki.

Annealing was performed in a quartz-tube furnace (pressure below 2×10^{-4} Pa) at temperatures from 900°C to 1100°C. The annealing time varied from 30 min to 19 h.

The Raman spectra were recorded in the 100–2800 cm^{-1} region by using a single-stage spectrometer (Acton SpectraPro 500I) in a low-resolution mode (~10 cm^{-1}) equipped with a 1024×256 pixel CCD camera (Andor InstaSpec IV). The 514.5-nm radiation of an Ar^{+} laser (Omnichrome 543-AP) was directed to a sample at 45° in P-polarization and focused to a ~50-μm spot, the laser power being ~50 mW. The Raman scattering light was transmitted to the spectrometer through a collecting optics, a holographic filter (Kaiser Super-Notch-Plus), and an optical fiber. In order to characterize the Raman spectra numerically, conventional two-Gaussian decomposition of the dominating spectral feature to D and G lines with a suitable background is used, which provides information on sp^2 clusterization. The peak width corresponds to the Gaussian parameter in $\exp(-2(x-x_0)^2/\sigma^2)$. In addition, we analyze the Raman intensity ratio $R = I_{500}/I_{1550}$ and the slope $S = (I_{1300} - I_{1100})/I_{1100}$, correlating with an sp^3 fraction η of DLC [19,20]. I_{500}, I_{1100}, I_{1300} and I_{1550} are Raman intensities at 500, 1100, 1300 and 1500 cm^{-1}, respectively.

The depth profiling of Si atoms was carried out by secondary ion mass spectrometry at the Technical Research Centre of Finland using a double focusing magnetic sector SIMS (VG Ionex IX70S). The current of the 5-keV O_2^{+} primary ions was typically 400 nA during depth profiling and the ion beam was raster-scanned over an area of 270×430 μm^2. Crater wall effects were avoided by using a 10% electronic gate and 1 mm optical gate. The pressure inside the analysis chamber was 5×10^{-8} Pa during the analysis. The depth of the craters was measured by a profilometer (Dektak 3030ST). The uncertainty of the crater depth was estimated to be 5%. The Si concentration of the as-implanted silicon profile was normalized to the implanted dose.

3. Results and discussion

Fig. 1 presents Raman spectra of DLC films, and Fig. 2 shows the extracted Raman parameters as a function of the annealing temperature. The Raman spectra of the as-deposited films display a D/G ratio of 0.4, G-line position at 1566 cm^{-1}, D-line position at 1350 cm^{-1}, $R = 0.33$, and $S = 0.55$ yielding $\eta \sim 30\%$.

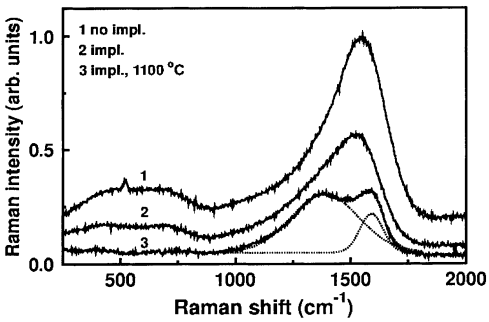

Fig. 1. Raman spectra of DLC films of non-implanted sample (line 1), implanted sample (line 2), implanted and annealed at 1100°C for 1 h (line 3). The conventional decomposition of the dominating feature to the D and G lines is shown (the dotted lines).

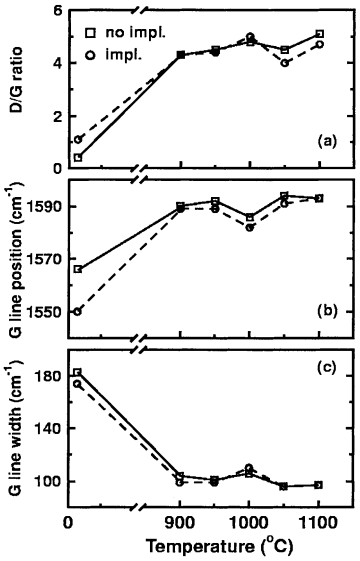

Fig. 2. Raman parameters of DLC films as a function of annealing temperature. The data are presented for the films without (squares) and with implantation (circles).

When Si is implanted into DLC, the G line shifts down in energy to 1550 cm^{-1} and narrows, D/G ratio increases to 1.1 and R and S parameters are 0.30 and 0.90, respectively. The behavior under ion implantation shows an increase of sp^2-coordinated clusters and decrease of the sp^3-ratio to ~10% which qualitatively corresponds to the related literature data [15–17]. Under annealing above 900°C, an efficient graphitization process is evidenced by up-shifting and narrowing of the G line and increasing of the D/G ratio (see Fig. 2). As evidenced by Raman spectra, the annealed material is totally sp^2-coordinated and no difference in film structure was observed in the annealing temperature region from 900°C to 1100°C as well as between the implanted and

non-implanted samples. Furthermore, small Si crystallites, if they are present, should be easily observable by a Raman scattering band in the 510–520 cm^{-1} region [21]. Weak peaks at ~520 cm^{-1} appearing occasionally in our spectra are rather applicable to the Si crystalline substrates because they do not show a systematic dependence on the annealing temperature. The Raman spectrum of a Si-doped carbon films on an Al substrate, studied earlier [22], displays no Si crystallites hence supporting this conclusion. We did not observe a formation of Si crystallites during annealing, which suggests the absence of extensive (>2 nm) clusterization of Si atoms in annealing up to 1100°C. On the other hand, amorphous Si grains are more difficult to detect in Si–C films because the corresponding phonon band is very broad. Amorphous Si structure can crystallize at about 1100°C even if their size is below 2 nm [23,24]. Zaharias et al. [25] reported crystallization of 3-nm-thick Si amorphous layers at 1100°C and crystallization of 5 nm layers below 1050°C. These data give the upper limit of sizes for amorphous Si grains that are possible in essential amount in our films.

The diffusion coefficients for silicon diffusion in amorphous carbon were determined by the use of the concentration independent diffusion equation

$$\frac{\partial C}{\partial t} = D\frac{\partial^2 C}{\partial x^2}, \tag{1}$$

where C is the concentration of Si, D diffusion coefficient, x depth from the surface, and t is the diffusion time. Eq. (1) was solved numerically with the as-implanted Si concentration profile as an initial distribution. The diffusion coefficient for every temperature was determined by a weighted least-squares fitting. The fitting was done by searching the diffusion coefficient in Eq. (1) that minimizes the weighted square error of an annealed profile

$$\mathrm{Err} = \sum_i \frac{(C_i - C_{\mathrm{exp}})^2}{C_{\mathrm{exp}}}, \tag{2}$$

where C_i and C_{exp} are the numerical and experimental concentrations at the same depth, respectively. The result of the fitting to a Si profile after annealing at 1100°C for 1 h is presented in Fig. 3. The Gaussian-like broadening of the as-implanted profile can be observed. The numerical fit agrees with the SIMS profile. Also plotted in the figure is the implantation-induced defect distribution simulated by SRIM-98. This deposited energy curve shows that the implanted Si loses most of its energy in the near-surface region. The symmetric broadening of the Si profile during annealing, however, leads us to the conclusion that implantation-induced and -annealed defects in this region do not significantly change the diffusion process from that observed in the deeper region.

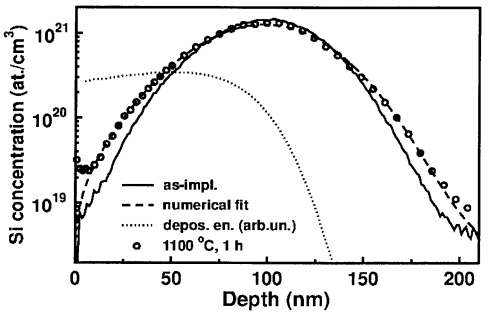

Fig. 3. Experimental concentration profile of Si obtained after annealing of DLC samples at 1100°C for 1 h, together with the numerical fit. The solid line shows the as-implanted Si profile. The dotted line is the deposited energy calculated by SRIM-98.

The results presented in Fig. 4 show Arrhenius behavior for Si diffusion with the following values for the activation energy E_a and pre-exponential factor D_0: $E_a = 1.6 \pm 0.1$ eV, $D_0 = 1.9 \times 10^{4\pm1}$ nm^2 s^{-1}. The values of the diffusion coefficients presented in Fig. 4 were 2.4×10^{-3}, 8.0×10^{-3}, 1.1×10^{-2}, 1.6×10^{-2} and 2.9×10^{-2} nm^2 s^{-1} at 900°C, 950°C, 1000°C, 1050°C and 1100°C, respectively. Experiments on carbon self-diffusion in pyrolitic graphite show that no diffusion takes place during annealing at 1150°C for 10 min [26]. The process occurred only after irradiation by 20-keV D^+ ions to a flux of 8×10^{15} ions cm^{-2} s^{-1}. Review of data on self-diffusion in graphite showed that the process is characterized by an activation energy of ~7 eV [27].

In order to compare our data for Si diffusion in amorphous carbon films with literature data for Si diffusion in matrix with similar electronic structure of atoms (four outer electrons), results on Si self-diffusion in crystalline matrix were considered [28]. They show that

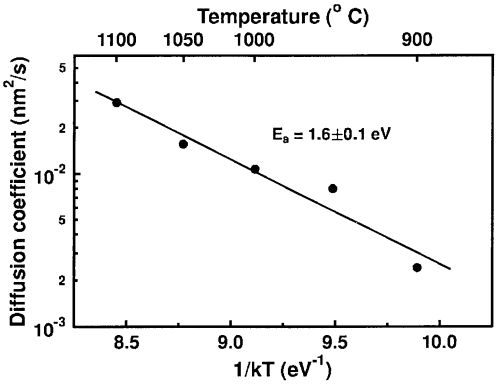

Fig. 4. Arrhenius plot for the diffusion coefficient of Si. Shown are the natural logarithms of the diffusion coefficients vs. $1/kT$, where k is Boltzmann's constant. The solid line is the fit to the experimental data.

the process proceeds mostly through self-interstitials. An activation energy of 4.75 ± 0.04 eV reported by H. Bracht et al. [28] is higher than the one found in the current study. The difference can be explained by the fact that the energy barrier needed for the diffusion jump is much higher in crystals than in amorphous materials. For self-diffusion in amorphous Si a range of activation energies indicating the multiplicity of mechanisms is found, the values vary from 0.23 to 2.7 eV [29,30]. In spite of the difference in materials the current value for the activation energy is in a better agreement with the limits reported for the amorphous Si than the value obtained for the crystalline Si.

Moro et al. [31] estimated the diffusion coefficient of Si in silicon carbide at 900°C to be 4.8×10^{-15} cm^2 s^{-1}. This value is much higher than the one shown in Fig. 4 for the same temperature. The discrepancy can be explained by the difference in the studied materials. An activation energy of 1.17 eV was obtained by using diffusion coefficients at 900°C [31] and at 1250°C [32]. This value is consistent with the results presented in the current study. However, it is hard to make a comparison since only two diffusion coefficients were considered.

4. Conclusion

Annealing behavior of $^{30}Si^+$-ion-implanted carbon films has been studied. No Si crystallites are formed in annealing, which suggests the absence of extensive (>2 nm) clusterization of Si atoms at thermal treatment up to 1100°C. The diffusion coefficients exhibit a good Arrhenius behavior with an activation energy and pre-exponential factor of 1.6 ± 0.1 eV and $1.9 \times 10^{4\pm1}$ nm^2 s^{-1}, respectively.

Acknowledgements

This work was supported in part by the Academy of Finland (Projects No. 45 090 130 and 46 798) and by the Association Euratom-TEKES. Authors want to thank Mr J. Kolehmainen and Mr J. Partanen (DIARC-Technology Inc.) for sample preparation.

References

[1] S.M. Sze, Physics of Semiconductor Devices, Wiley, New York, 1981, pp. 790–838.
[2] S.A. Kajihara, A. Antonelli, J. Bernholc, R. Carr, Phys. Rev. Lett. 66 (1991) 2010.
[3] M. Balden, J. Roth, C.H. Wu, J. Nucl. Mater. 258–263 (1998) 740.
[4] M. Yoshikawa, Mater. Sci. Forum 52–53 (1989) 365.
[5] C.Z. Wang, K.M. Ho, Phys. Rev. Lett. 71 (1993) 1184.
[6] D.A. Drabold, P.A. Fedders, P. Stumm, Phys. Rev. B 49 (1994) 16415.
[7] D.G. McCulloch, S. Prawer, A. Hoffman, Phys. Rev. B 50 (1994) 5905.
[8] D.M.P. Nadler, T.M. Danovan, A.K. Green, Thin Solid Films 116 (1984) 241.
[9] J. Wagner, M. Ramsteiner, C. Wild, P. Koidl, Phys. Rev. B 40 (1989) 1817.
[10] J. Robertson, Prog. Solid State Chem. 21 (1991) 199.
[11] J.C. Knight, T.F. Page, H.W. Chandler, Surf. Coat. Technol. 49 (1991) 519.
[12] D.R. Tallant, J.E. Parmeter, M.P. Siegal, R.L. Simpson, Diamond Relat. Mater. 4 (1995) 191.
[13] S. Anders, J. Diaz, J.W. Ager III, R. Yu Lo, D.B. Bogy, Appl. Phys. Lett. 71 (1997) 3367.
[14] R. Kalish, Y. Lifshitz, K. Nugent, S. Prawer, Appl. Phys. Lett. 74 (1999) 2936.
[15] D.G. McCulloch, E.G. Gerstner, D.R. McKenzie, S. Prawer, R. Kalish, Phys. Rev. B 52 (1995) 850.
[16] D.G. McCulloch, D.R. McKenzie, S. Prawer, A.R. Merchant, E.G. Gerstner, R. Kalish, Diamond Relat. Mater. 6 (1997) 1622.
[17] A. Stanishevsky, L. Khriachtchev, J. Appl. Phys. 86 (1999) 7052.
[18] E. Vainonen, J. Likonen, T. Ahlgren, P. Haussalo, J. Keinonen, C.H. Wu, J. Appl. Phys. 82 (1997) 3791.
[19] L. Khriachtchev, R. Lappalainen, M. Hakovirta, M. Räsänen, Diamond Relat. Mater. 6 (1997) 694.
[20] A. Stanishevsky, L. Khriachtchev, R. Lappalainen, M. Räsänen, Diamond Relat. Mater. 6 (1997) 1026.
[21] Ch. Ossadnik, S. Veprek, I. Gregora, Thin Solid Films 337 (1999) 148 and references therein
[22] L. Khriachtchev, E. Vainonen-Ahlgren, T. Sajavaara, T. Ahlgren, J. Keinonen, J. Appl. Phys. 88 (2000) 2118.
[23] P.D. Persans, A. Ruppert, B. Abeles, J. Non-Cryst. Solids 102 (1988) 130.
[24] L. Khriachtchev, M. Räsänen, S. Novikov, O. Kilpelä, J. Sinkkonen, J. Appl. Phys. 86 (1999) 5601.
[25] M. Zaharias, J. Bläsing, P. Veit, L. Tsybeskov, K. Hirschman, P.M. Fauchet,, Appl. Phys. Lett. 74 (1999) 2614.
[26] B. Soder, J. Roth, W. Moller, Phys. Rev. B 37 (1988) 815.
[27] P.A. Thrower, R.M. Mayer, Phys. Status Solidi A 47 (1978) 11.
[28] H. Bracht, E.E. Haller, Phys. Rev. Lett. 81 (1998) 393.
[29] S. Roorda, W.C. Sinke, J.M. Poate, D.C. Jacobson, S. Dierker, B.S. Dennis, D.J. Eaglesham, F. Spaepen, P. Fuoss, Phys. Rev. B 44 (1991) 3702.
[30] J.H. Shin, H.A. Atwater, Phys. Rev. B 48 (1993) 5964.
[31] L. Moro, A. Paul, D.C. Lorents, R. Malhotra, R.S. Ruoff, P. Lazzeri, L. Vanzetti, A. Lui, S. Subramoney, J. Appl. Phys. 81 (1997) 6141.
[32] J. Graul, E. Wagner, Appl. Phys. Lett. 21 (1972) 67.